**Tech Science Press**

# A Numerical Investigation into the Influence of Electrode-Related Parameters on Electroosmotic Mixing and Related Mechanisms

## Chunsheng Wang[*] and Dongxing Shang

College of Vehicles and Energy, Yanshan University, Qinhuangdao, 066000, China
*Corresponding Author: Chunsheng Wang. Email: wangcs@ysu.edu.cn

**Abstract:** Electroosmosis is an effective method for liquid mixing. It is associated with the motion of a liquid in a microchannel induced by an applied electric field. In this manuscript, a numerical model is elaborated and implemented for the case of a straight channel with a single electrode pair. In particular, the Navier-Stokes equation combined with the Convection-diffusion and Helmholtz-Smoluchowski equation are used to simulate the resulting flow field. The influence of various electrode parameters on the mixing efficiency and the related mechanisms are investigated. The numerical results show that a pair of eddies are produced alternately by the changing electric field. The two liquids are mixed by the interaction of this pair of eddies. The length of the electrode affects the distance between these eddies, while the amplitude and frequency of electrode voltage determine the intensity and frequency of the eddy current, respectively. It is shown that by tuning properly the electrode parameters, the mixing efficiency can reach 97.5%. The optimization process implemented in the present work may lead in the future to a new approach to obtain controllable electroosmotic flow in microfluidic platforms.

## 1 Introduction

Introduction of external electric fields into electrolyte diffusion can drive the flow of liquid on the wall, thus forming electroosmotic flows [1]. The electroosmotic flows provide an active strategy to solve a variety of flow issues [2–5]. Especially in the field of biochemical reactions [6], it is essential to generate a homogenous mixture rapidly after the initial reaction. Microfluidic reactors using electroosmotic technology can provide faster uniform mixing and higher yields than conventional reactors [7–9].

Researches on electroosmosis mixing have been carried out on different channel structures. For rectangular channel, the instantaneous electroosmotic flow is simulated and the relationship between the flow field and applied electric field is also given [10–12]. Zhuang et al. [13,14] studied the influence of electro-osmotic driving flow on the mixing of power-law fluid in T-shaped micro-channels. Wu [15] studied the nonlinear mixing process in Y-type micro-channels. Rahim [16] designed a Y-mixer and a Y-shaped chute mixer, and corresponding researches show that the Y-shaped mixer at the bottom of the mixing channel has a more significant mixing effect. To enhance electroosmotic mixing in a

microchannel, a periodically varying electroosmotic flow is generated to control the size and direction of the electroosmotic flow by manipulating either the distribution of zeta potential at the wall or the applied external electric field [17–19].

Further researches have focused on the factors affecting the mixing efficiency, such as electrode characteristics [20,21], fluid temperature [22], liquid viscosity [23] and ion concentration [24]. Alizadeh et al. studied the distribution characteristics of electric field and the velocity of electroosmotic flow by the lattice Poisson-Boltzmann method [25–27] investigated the optimum range of electroosmosis parameters. The results showed it can lead to a highly efficient mixer by increasing disturbances in the primary laminar flow.

The previous works mainly focus on the design of mixers with complex structures and the influence of single parameter on mixing efficiency. In this work, we focus on the influence mechanism of electrode parameters on the mixing efficiency. The effect of electrode parameters on electroosmotic flow and mixing efficiency is revealed. Furthermore, the global optimal mixing efficiency based on electrode parameters is given by numerical optimization algorithm.

## 2 Model and Numerical Results

### 2.1 Physical Model

The structure of straight channel micro-mixer is shown in Fig. 1. Two liquids flow into the mixer from inlets $A_1$ and $A_2$, respectively. Mixed liquids leave the micro-mixer from outlet $A_3$. The widths of $A_1$ and $A_2$ are both 5 μm. The length of straight channel L = 100 μm. A pair of electrodes are set on the upper and lower walls of the channel, with the electrode length W = 5 μm. And the distance between the left boundary of the electrode and the entrance of the channel is 30 μm.
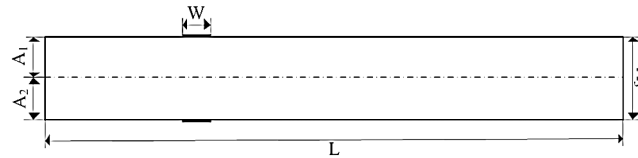


**Figure 1:** Structure of micro-mixer

The Navier-Stokes equation [28] for incompressible flow is used to describe the flow field in the micro-channel:

$$\nabla \cdot u = 0$$

$$\rho \frac{\partial u}{\partial t} - \nabla \cdot \eta (\nabla u + \nabla u^T) + \rho u \cdot \nabla u + \nabla p = 0 \tag{1}$$

Inside the mixer, the following convection-diffusion equation is applied to account for the concentration of the dissolved substances in the fluid:

$$\frac{\partial c}{\partial t} + \nabla \cdot (-D\nabla c) + u \cdot \nabla c = 0 \tag{2}$$

where, the fluid velocity at the entrance u = 0.2 mm/s; the pressure at the outlet is set to a standard atmospheric pressure; c is the fluid concentration, at the upper half of the inlet, the solute has a given concentration 1 mol/m$^3$, the concentration at the lower half is 0; the fluid density $\rho$ = 1000 kg/m$^3$; the dynamic viscosity coefficient $\eta$ = 10$^{-3}$ pa·s; the fluid diffusion coefficient D = 10$^{-11}$ m$^2$/s.

A sinusoidal voltage with amplitude of 0.1 V and frequency of 10 Hz is loaded on the electrodes. The fluid velocity on the wall is described by Helmholtz-Smoluchowski equation, as [21]

$$u_w = \frac{\varepsilon_w \zeta_0}{\eta} \nabla_T V \qquad (3)$$

where, $\nabla_T V$ is the tangential component of the electric field; $\varepsilon_\omega = \varepsilon_0 \cdot \varepsilon_r$ is the permittivity (F/m), relative electric permittivity $\varepsilon_r = 80.2$; the zeta potential at the channel wall $\zeta_0 = -0.1$V.

Based on the above physical parameters and boundary conditions, for the quantitative evaluation of mixing performance, the mixing efficiency at the profile of the outlet $A_3$ is introduced as [27]:

$$\eta = 1 - \frac{\int_{A3}|C - C_\infty|}{\int_{A3}|C_0 - C_\infty|} \qquad (4)$$

where, C is the concentration of mixed fluid; $C_\infty$ and $C_0$ are the concentrations associated with fully mixed and completely unmixed states, respectively.

### 2.2 Numerical Results

The mixing efficiency at the outlet of micro-channel varies with time is shown in Fig. 2. The numerical result shows after the flow delay of 0.2 s, the mixing efficiency increases gradually, and finally presents periodic fluctuation with small amplitude. The disturbance caused by the electroosmosis electric field initially occurs near the electrodes. The disturbed flow field reaches the outlet of the channel at the time of 0.2 s, and after 0.8 seconds, a stable flow field is formed. The average mixing efficiency is about 94%, and the fluctuation frequency of mixing efficiency is equal to that of the electroosmotic voltage.

In order to investigate the effect of electric field on flow field, streamlines and concentration distribution of steady flow are given in Fig. 3. When the phase angle of sinusoidal voltage is 90°, the voltage between upper electrode and lower electrode is 0.1 V. Under the influence of electric field, a pair of eddies are produced at the left edge of the upper electrode and the right edge of the lower electrode. The eddy structure disturbs the flow field, and transfers the liquid from the lower part to the upper part of the channel (Fig. 3a). The characteristics of the eddies produced at the edge of the electrode are consistent with existing studies [8]. After this time point, the strength of eddies decreases with the decrease of the electric field. When the applied voltage is 0, the pair of eddies disappear (Fig. 3b). As the sinusoidal
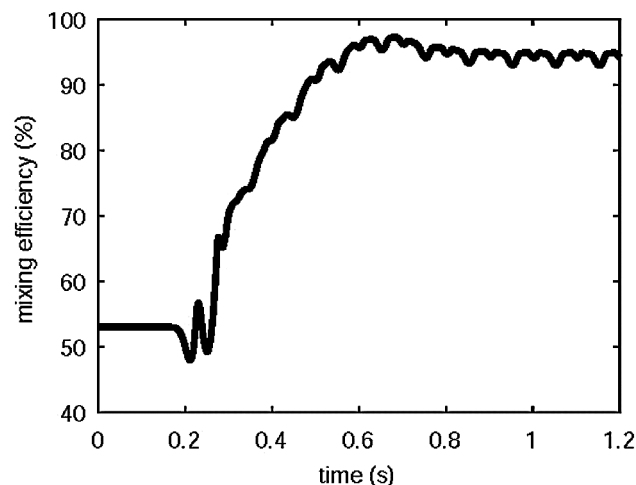
**Figure 2:** Change of mixing efficiency with time
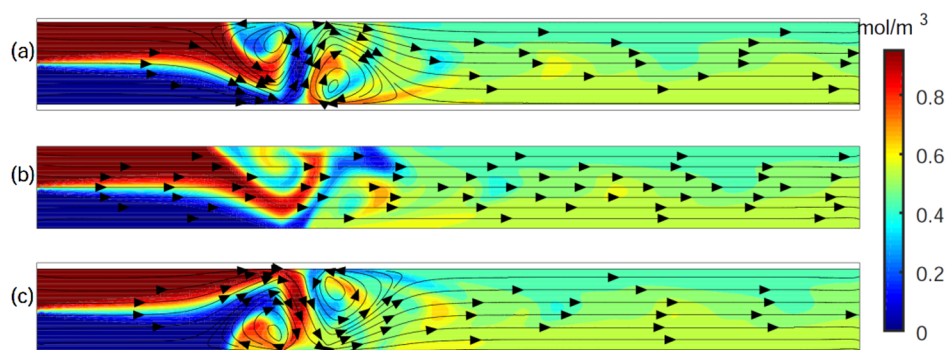
**Figure 3:** Streamlines and concentration distribution of fluid at different phase angles of voltage ((a) 90°, (b) 180°, (c) 270°)

voltage becomes negative with the pass of time, another pair of eddies forms and the disturbance direction of fluid changes. As shown in Fig. 3c, the liquid from the upper part of the channel is carried to the lower part of the channel.

In consequence, as the voltage value changes positively and negatively, two pairs of eddies alternately appear and disturb the liquid in the different directions, thus realizing the active mixing of the two liquids.

## 3 Effect of Electrode Parameters on the Mixing Efficiency

The parameters of electrode will affect the eddy characteristics and the mixing efficiency. Effect mechanisms of electrode parameters on the mixing efficiency will be analyzed in this section.

### 3.1 Effect of Voltage Amplitude

The voltage amplitude of the electrode changes from 0.05 to 0.15 V, and the average mixing efficiency is obtained after the flow is stable (Fig. 4). Numerical simulations show the mean mixing efficiency increases first and then decreases slightly with the increase of voltage amplitude.
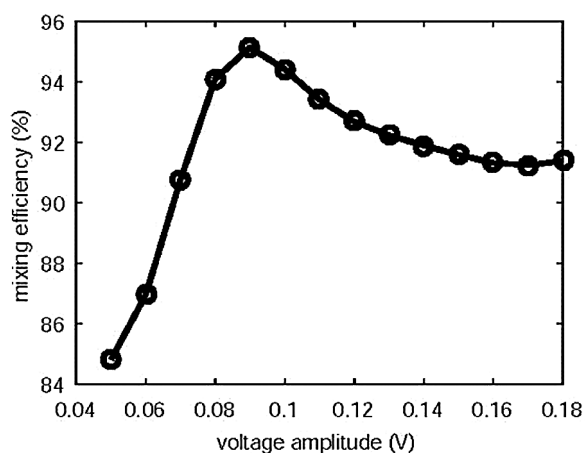


**Figure 4:** Change of mean mixing efficiency with voltage amplitude

Keeping the phase angle of voltage at 90°, the distribution of flow field and concentration field in the channel at the electrode voltage of 0.06 V and 0.14 V is shown in Fig. 5. When the voltage amplitude of the electrodes is small, the intensity of the eddy formed by electroosmosis is small, thus the ability of the
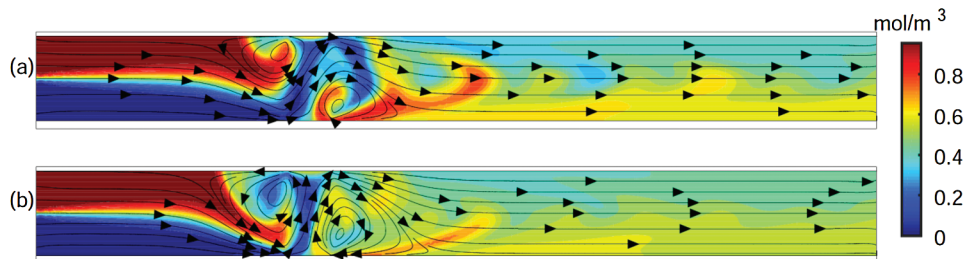
**Figure 5:** Streamlines and concentration distribution at different voltage amplitude ((a) voltage of 0.06 V, (b) voltage of 0.14 V)

eddy to disturb the liquid is weak, the liquids are not mixed sufficiently. On the other hand, when the voltage of the electrodes is larger than 0.09 V, a pair of large eddies will squeeze the liquid of low concentration and form a backflow in the upper eddy. Excessive low concentration liquid is transported to the upper part of the channel, which reduces the mixing efficiency. Therefore, the magnitude of the voltage determines the strength of the eddy and the movement of the fluid between the two eddies, which affects the mixing efficiency ultimately.
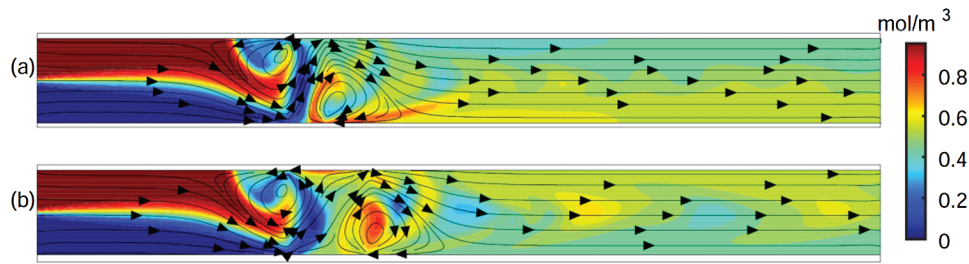
### 3.2 Effect of Electrode Length

Keep the position of the left boundary of the electrode fixed and change the length of the electrode. The change of mean mixing efficiency is shown in Fig. 6. The numerical results show that the mixing efficiency increases first and then decreases with the increase of electrode length. When the electrode length is 6.5–7.5 μm, the mixing efficiency reaches a higher value, about 96%.
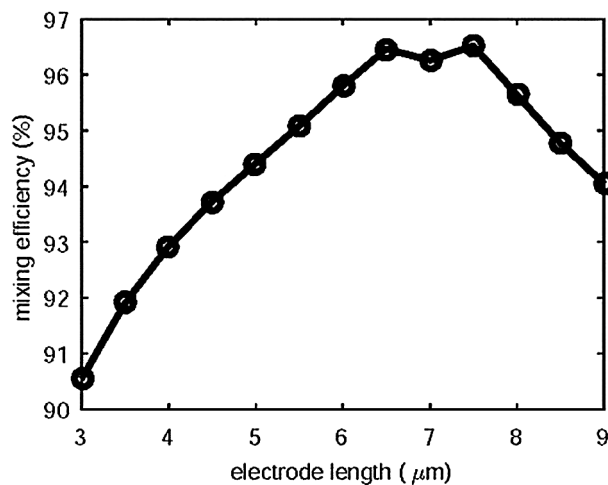


**Figure 6:** Change of mean mixing efficiency with electrode length

When the phase angle of the electrode voltage is 90°, the effects of the electrode length on the flow field and concentration field are shown in Fig. 7. When the length of the electrode is 4 μm, eddies generated on the upper and lower walls are relatively close. Similar to the case of high voltage (Fig. 5b), the fluid in the lower part of the channel is driven to the upper wall. Due to excessive transport intensity, liquid mixing efficiency decreases. For the case where the electrode length is 9 μm, increased distance between the two electrodes results in a decrease of the interaction intensity between them. Fig. 7b shows that the fluid in the upper
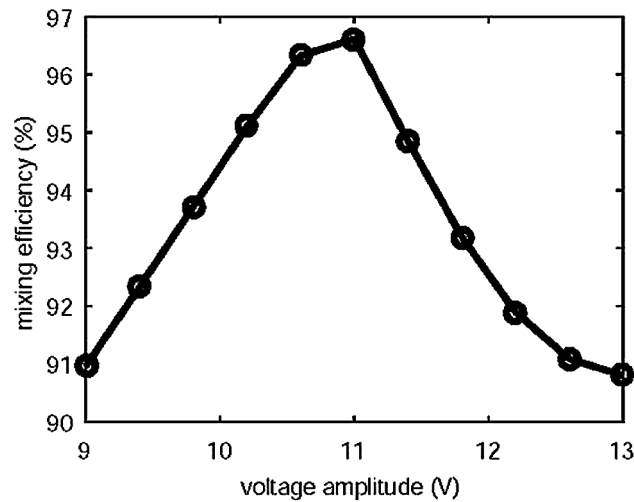
**Figure 7:** Streamlines and concentration distribution at different electrode length ((a) electrode length of 4 μm, (b) electrode length of 9 μm)

eddy failed to be carried downstream by the lower eddy. Therefore, the distance between eddies affects the coupling strength and mixing efficiency.

### 3.3 Effect of Voltage Frequency

Furthermore, the mixing efficiency is investigated with changing the frequency of the electrode power (Fig. 8). Numerical results show when the frequency is about 11 Hz, the mixed frequency reaches a maximum value.



**Figure 8:** Change of mean mixing efficiency with voltage frequency

When the phase angle of the electrode voltage is 90°, the streamlines and concentration distribution at the frequency of 9.8 Hz and 11.8 Hz are shown in Fig. 9. In both cases, the flow field structures are similar while the concentration fields are different. With low frequency of voltage (Fig. 9a), the eddy current lasts for a long time and a large amount of liquid at the bottom of the channel is transported to the upper part of the channel. Therefore, at the outlet of the channel, the concentration of the upper portion is low while the concentration of the lower portion is high. When the voltage frequency is higher, transport capacity of fluid decreases owing to the rapid change of flow field. The liquid concentration in the upper part of the channel is higher than that in the lower part. There is an optimal frequency to make the concentration at the outlet of the channel more uniform.
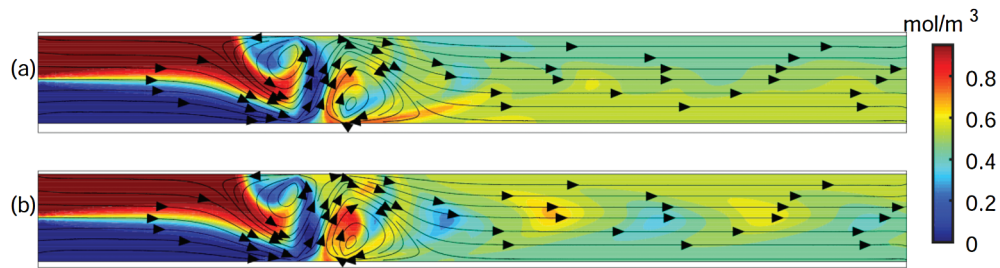
**Figure 9:** Streamlines and concentration distribution at different voltage frequency ((a) frequency of 9.8 Hz, (b) frequency of 11.8 Hz)

## 4 Optimization of Electrode Parameters

The numerical results show that there are optimum parameters for the electrode voltage, electrode length and frequency under the condition of single parameter changes. In order to achieve the highest mixing efficiency in the global scope, the numerical algorithm of global search is used to optimize the three electrode parameters [29]. The range of electrode parameters and the final optimum values are shown in Tab. 1. With the optimum electrode parameters, the mixing efficiency is up to 97.5%.

**Table 1:** The parameters of being optimized

| Parameter Name | Parameter range | Optimum value |
| --- | --- | --- |
| Voltage amplitude | 0.05–0.18 V | 0.087 V |
| Electrode length | 3–9 μm | 7.06 μm |
| Voltage frequency | 9–13 Hz | 9.7 HZ |

## 5 Conclusion

The influence mechanism of electroosmotic parameters on the mixing efficiency is studied by a numerical model of straight channel mixer. Compared with the existing research, the parameter of electrode length is introduced in this manuscript, which affects the position of eddy current, thus enhancing the ability to control the flow field greatly.

In summary, a pair of eddies are produced alternately at the edges of electrodes under the effect of electroosmotic voltage. From these results, we conclude that the length of electrode affects the distance between eddies, the amplitude and frequency of electrode voltage determine the intensity and frequency of eddy current, respectively. Therefore, changes in electrode parameters can modify the characteristics of eddy current, which in turn affects the mixing efficiency. By optimizing the electrode parameters, the mixing efficiency can reach 97.5% in the simplest structure of mixer.

Electroosmotic mixing has important application prospects. The research results can guide the design of electroosmotic mixer in straight channel, and the obtained analytical solution can be used as meaningful methods to improve the mixing efficiency in microfluidic systems.

**Conflicts of Interest:** The authors declare that they have no conflicts of interest to report regarding the present study.

**References**

 1. Yang, D. Y., Wang, Y. (2015). Effects of ion concentration on electroosmotic flow and micromixing in microchannels. *Applied Mathematics & Mechanics, 36(9),* 981–989.

 2. Kim, S. J., Yoon, B. J. (2019). Analytical study of AC electroosmotic mixing in 2-dimensional microchannel with time periodic surface potential. *Biomicrofluidics, 13(2),* 024102. DOI 10.1063/1.5091936.

 3. Sugioka, H. (2016). Suppression of a Brownian noise in a hole-type sensor due to induced-charge electro-osmosis. *Physics of Fluids, 28(3),* 032003. DOI 10.1063/1.4943495.

 4. Lauricella, M., Cipolletta, F., Pontrell, G. (2017). Effects of orthogonal rotating electric fields on electrospinning process. *Physics of Fluids, 29(8),* 082003. DOI 10.1063/1.4997086.

 5. Mohammadi, M., Madadi, H., Casals-Terre, J. (2015). Microfluidic point-of-care blood panel based on a novel technique: reversible electroosmotic flow. *Biomicrofluidics, 9(5),* 054106. DOI 10.1063/1.4930865.

 6. Tawfiq, C., Brahim, D., Rachid, K. (2017). Computational investigation of droplets behaviour inside passive microfluidic oscillator. *Fluid Dynamics & Materials Processing, 13(3),* 173–187.

 7. Seong-Geun, J., Jae-Hoon, J., Kyoung-Ku, K., Hyung, J. S., Byungjin, L. (2018). Nanoliter scale microloop reactor with rapid mixing ability for biochemical reaction. *Korean Journal of Chemical Engineering, 37(10),* 2036–2042.

 8. Zhang, K., Ren, Y., Hou, L., Feng, X., Chen, X. (2018). An efficient micromixer actuated by induced-charge electroosmosis using asymmetrical floating electrodes. *Microfluidics and Nanofluidics, 22(11),* 130. DOI 10.1007/s10404-018-2153-2.

 9. Elvira, K. S., Solvas, I. X. C., Wootton, R. C. R. (2013). The past, present and potential for microfluidic reactor technology in chemical synthesis. *Nature Chemistry, 5(11),* 905–915. DOI 10.1038/nchem.1753.

10. Yang, D. Y., Liu, Y. (2009). Numerical simulation of electroosmotic flow in hydrophobic microchannels. *Science in China Series E: Technological Sciences, 52(8),* 2460–2465. DOI 10.1007/s11431-008-0300-9.

11. Luo, W. J., Pan, Y. J., Yang, R. J. (2005). Transient analysis of electro-osmotic secondary flow induced by dc or ac electric field in a curved rectangular microchannel. *Journal of Micromechanics and Microengineering, 15(3),* 1–11. DOI 10.1088/0960-1317/15/1/001.

12. Hadigol, M., Nosrati, R., Nourbakhsh, A., Raisee, M. (2011). Numerical study of electroosmotic micromixing of non-Newtonian fluids. *Journal of Non-Newtonian Fluid Mechanics, 166(17),* 965–971. DOI 10.1016/j.jnnfm.2011.05.001.

13. Zhuang, Y., Zhu, Q. (2015). Numerical study of mixed electroosmotic pressure driven flow of power-law fluids in T-shaped micro-channels. *Procedia Engineering, 126,* 740–744. DOI 10.1016/j.proeng.2015.11.282.

14. Erickson, D., Li, D., Park, C. B. (2002). Numerical simulations of capillary-driven flows in nonuniform cross-sectional capillaries. *Journal of Colloid and Interface Science, 250(2),* 422–430. DOI 10.1006/jcis.2002.8361.

15. Wu, Z. G., Nguyen, N. T., Huang, X. Y. (2004). Nonlinear diffusive mixing in microchannels: theory and experiments. *Journal of Micromechanics and Microengineering, 14(4),* 604–611. DOI 10.1088/0960-1317/14/4/022.

16. Rahim, S. A., Ibrahim, T. N. T., Ma'Radzi, A. A., Jamil, M. M. A. (2014). Design and development of oblique groove micromixer for laminar blood reagent mixing. *IEEE International Conference on Control System, Computing and Engineering*, pp. 547–550.

17. Tada, S., Omi, Y., Eguchi, M. (2018). Analysis of the dielectrophoretic properties of cells using the isomotive AC electric field. *Biomicrofluidics, 12(4),* 044103. DOI 10.1063/1.5031054.

18. Chang, C. C., Yang, R. J. (2007). Electrokinetic mixing in microfluidic systems. *Microfluidics and Nanofluidics, 3(5),* 501–525. DOI 10.1007/s10404-007-0178-z.

19. Jiang, H., Weng, X., Li, D. (2014). A novel microfluidic flow focusing method. *Biomicrofluidics, 8(5),* 054120. DOI 10.1063/1.4899807.

20. Zhang, Y. T., Chen, H., Mezic, I., Meinhart, C. D., Petzold, L. et al. (2004). SOI processing of a ring electrokinetic chaotic micromixer. *Lubrication Engineering, 1,* 292–295.

21. Nayak, A. K. (2014). Analysis of mixing for electroosmotic flow in micro/nano channels with heterogeneous surface potential. *International Journal of Heat and Mass Transfer, 75,* 135–144. DOI 10.1016/j.ijheatmasstransfer.2014.03.057.

22. Alizadeh, A., Zhang, L., Wang, M. (2014). Mixing enhancement of low-Reynolds electro-osmotic flows in microchannels with temperature-patterned walls. *Journal of Colloid and Interface Science, 431,* 50–63. DOI 10.1016/j.jcis.2014.05.070.

23. Yang, D. Y. (2011). Numerical analysis of micro-mixing in rough microchannels. *Advanced Materials Research, 189–193,* 1452–1455. DOI 10.4028/www.scientific.net/AMR.189-193.1452.

24. Alizadeh, A., Wang, J. K., Pooyan, S., Mirbozorgi, S. A., Wang, M. (2013). Numerical study of active control of mixing in electro-osmotic flows by temperature difference using lattice Boltzmann methods. *Journal of Colloid and Interface Science, 407(10),* 546–555. DOI 10.1016/j.jcis.2013.06.026.

25. Wang, J., Wang, M., Li, Z. (2005). Lattice boltzmann simulations of mixing enhancement by the electro-osmotic flow in microchannels. *Journal Modern Physics Letters B, 19(28–29),* 1515–1518. DOI 10.1142/S0217984905009791.

26. Alipanah, M., Ramiar, A. (2017). High efficiency micromixing technique using periodic induced charge electroosmotic flow: a numerical study. *Colloids and Surfaces A: Physicochemical and Engineering Aspects, 524,* 53–65. DOI 10.1016/j.colsurfa.2017.04.020.

27. Jain, M., Nandakumar, K. (2010). Novel index for micromixing characterization and comparative analysis. *Biomicrofluidics, 4(3),* 031101. DOI 10.1063/1.3457121.

28. Frédéric, G., Chohong, M., Hector, D. (2007). Non-graded adaptive grid approaches to the incompressible Navier-Stokes equations. *Fluid Dynamics & Materials Processing, 3(1),* 37–48.

29. Conn, A. R., Scheinberg, K., Vicente, L. N. (2013). Introduction to derivative-free optimization. *MPS-SIAM Series on Optimization, 53(2),* 395–396.